Journal of Physics D: Applied Physics

PAPER

Degradation study of InGaN-based laser diodes grown on Si

To cite this article: Yongjun Tang *et al* 2020 *J. Phys. D: Appl. Phys.* **53** 395103

View the article online for updates and enhancements.

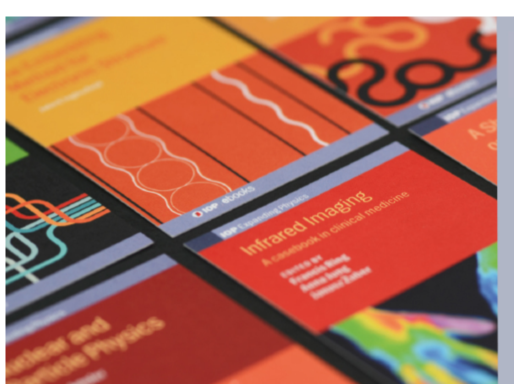

IOP ebooks™

Bringing together innovative digital publishing with leading authors from the global scientific community.

Start exploring the collection–download the first chapter of every title for free.

This content was downloaded from IP address 166.111.120.18 on 24/07/2020 at 12:34

IOP Publishing Journal of Physics D: Applied Physics

J. Phys. D: Appl. Phys. 53 (2020) 395103 (6pp) https://doi.org/10.1088/1361-6463/ab985f

Degradation study of InGaN-based laser diodes grown on Si

Yongjun Tang[1,2], Meixin Feng[1,2,3], Pengyan Wen[2], Jianxun Liu[2,3], Jin Wang[2], Xiujian Sun[2,3], Qian Sun[1,2,3], Shuming Zhang[1,2,3], Xing Sheng[4], Masao Ikeda[2] and Hui Yang[1,2,3]

[1] School of Nano-Tech and Nano-Bionics, University of Science and Technology of China, Hefei 230026, People's Republic of China
[2] Key Laboratory of Nanodevices and Applications, Suzhou Institute of Nano-Tech and Nano-Bionics, Chinese Academy of Sciences (CAS), Suzhou 215123, People's Republic of China
[3] Suzhou Institute of Nano-Tech and Nano-Bionics, CAS, Foshan 52800, People's Republic of China
[4] Department of Electronic Engineering, Beijing National Research Center for Information Science and Technology and IDG/McGovern Institute for Brain Research, Tsinghua University, Beijing 100084, People's Republic of China

E-mail: mxfeng2011@sinano.ac.cn, qsun2011@sinano.ac.cn and smzhang2010@sinano.ac.cn

Received 5 March 2020, revised 22 May 2020
Accepted for publication 1 June 2020
Published 9 July 2020

Abstract

The degradation characteristics of InGaN-based laser diodes (LDs) grown on Si substrate have been studied under an electrical stress with a pulsed current of 180 mA. After the electrical stress, the light output power, leakage current and capacitance of the LD decreased, while the operation voltage and threshold current increased, and the slope efficiency remained nearly unchanged after the pulsed electrical stress for 620 h. Further analysis shows that the degradation was probably due to the newly generated group-III vacancies and/or related defects, which can not only act as acceptor-like defects to compensate the n-type donors, leading to the reduction of conductance and capacitance, but also work as non-radiative recombination centers affecting the internal quantum efficiency and emission intensity of the active region.

Keywords: degradation, InGaN, laser diode, GaN-on-Si, group-III vacancies, dislocation

(Some figures may appear in colour only in the online journal)

1. Introduction

InGaN-based visible laser diodes (LDs) have attracted much attention due to wide applications in lighting, laser display and visible light communication [1–4]. However, most of the commercial InGaN-based LDs are grown on small-size, costly, free-standing GaN substrates, and hence are much more expensive than InGaN-based light emitting diodes [5, 6]. Compared with free-standing GaN substrates, Si substrates have apparent advantages in wafer size and material cost, and using Si substrate to grow InGaN based LDs can slash the device cost. More importantly, the emission wavelength of InGaN materials could be adjusted from visible band to infrared band, so, InGaN-based LDs grown on Si may be used as a potential on-chip light source for Si photonics [7, 8]. At present, the integration of III–V semiconductor LDs on Si by bonding is being adopted in some applications. However, the chip bonding process is difficultly compatible with wafer-level large-scale manufacturing foundries. Therefore, InGaN-based LDs directly grown on Si substrate have received wide attention.

However, there are several key challenges during the epitaxial growth of InGaN-based LDs on Si substrate due to the huge mismatch in both lattice constant and coefficient of thermal expansion (CTE) between GaN and Si, which often leads to the formation of a high density of threading dislocations (TDs) and crack network in the LD structure grown on Si [9]. With the insertion of AlN/AlGaN multi-layer buffer between GaN and Si substrate, the TD density in the crack-free overgrown LD structure was substantially reduced, resulting in the demonstration of electrically injected lasing operation at room temperature of the InGaN-based LDs grown on Si

 © 2020 IOP Publishing Ltd Printed in the UK

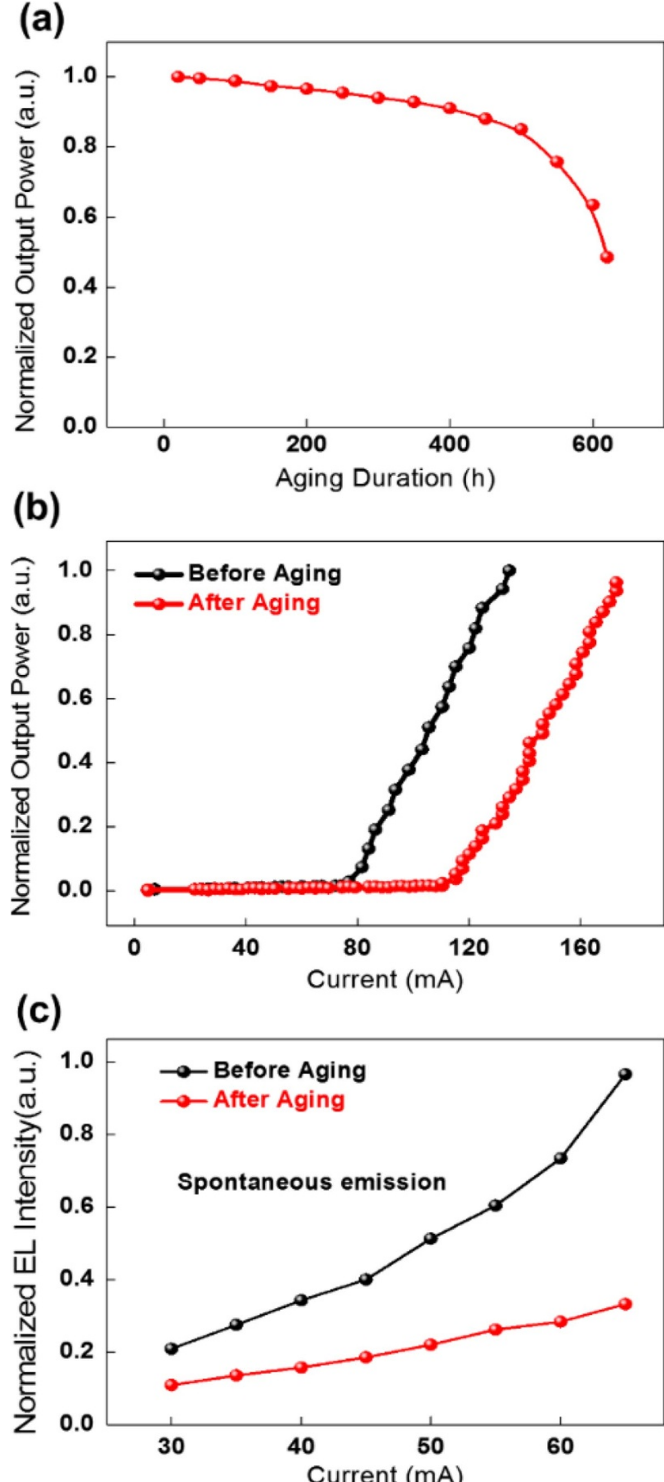

Figure 1. (a) The light output power of the LD as a function of aging duration. (b) The *L-I* curves and (c) the spontaneous emission integral intensity of the LD before and after aging.

[10, 11]. By suppressing the formation of point defects during the epitaxial growth of LDs, we recently further reduced the threshold current and voltage, as well as junction temperature, of the LDs [12]. But the operation lifetime of the as-fabricated LDs grown on Si was still quite limited. It is necessary to study the degradation mechanism of InGaN-based LDs grown on Si.

In this paper, we studied the degradation characteristics of the InGaN-based LDs grown on Si substrate under an electrical stress. As the aging duration increased, the threshold current increased, and the light output power decreased. Surprisingly, the leakage current and capacitance of the aged LD were also reduced, and the series resistance and operation voltage of the LD increased significantly. Moreover, the slope efficiency remained nearly unchanged after the pulsed electrical stress for 620 h. Further analysis indicates that the degradation of the LD could be attributed to the generation of group-III vacancies and/or related complexes in or around the active region of the LD during the electrical stress.

2. Experiments

The InGaN-based LDs were grown on Si substrate by metal organic chemical vapor deposition. The LD epitaxial structure was composed of an AlN/AlGaN multilayer buffer, a 1.3 μm-thick undoped GaN layer, a 1.3 μm-thick n-GaN contact layer, a 1.2 μm-thick n-$Al_{0.08}Ga_{0.92}N$ cladding layer (CL), three pairs of $In_{0.12}Ga_{0.88}N/In_{0.02}Ga_{0.98}N$ quantum wells sandwiched by $In_{0.02}Ga_{0.98}N$ and GaN waveguide layers, an 20 nm-thick p-$Al_{0.2}Ga_{0.8}N$ electron blocking layer, a 600 nm-thick p-$Al_{0.06}Ga_{0.94}N$ CL, and a 30 nm-thick p-GaN contact layer. The ridge etching depth was about 530 nm, and only about 100 nm-thick p-AlGaN CL was left. The ridge width and cavity length of the LD were 4 and 800 μm, respectively. In order to decrease threshold current, three and seven pairs of quarter-wave TiO_2/SiO_2 dielectric coatings were deposited on the front and the rear facets, respectively. More detailed LD structure could be found elsewhere [9]. The aged LD chips were still on the laser bar with no package, and the aging test was conducted under a constant pulsed current (180 mA) at room temperature in an air atmosphere. The pulse width and the repetition rate were 400 ns and 10 kHz, respectively.

The light output power was monitored by a photodiode during aging, and the light output power versus injection current (*L-I*) curves of the aged LD before and after aging were measured by a calibrated optical power meter (Thorlabs PM121D). The current-voltage (*I–V*) characteristics were measured by a continuous-wave power supply (Keithley 2400) at various aging duration. The spontaneous emission intensities were measured by a delicate photodiode before and after aging. The capacitance-voltage (*C–V*) characteristic of the LD was measured by a semiconductor parameter meter (Agilent B1500A). After the electrical characterization, the metal electrodes of LD were removed by aqua regia (V_{HCl}: V_{HNO3} = 3:1) prior to the of photoluminescence (*PL*) study of the LD under an excitation of a 405 nm laser source.

3. Results and discussions

Figure 1(a) shows the evolution of light output power of the LD under the electrical stress during the aging. In the first 400 h, the output power of the LD only showed a gradual decrease, but a rapid decay was observed as the aging duration further increased. When the aging duration reached 620 h,

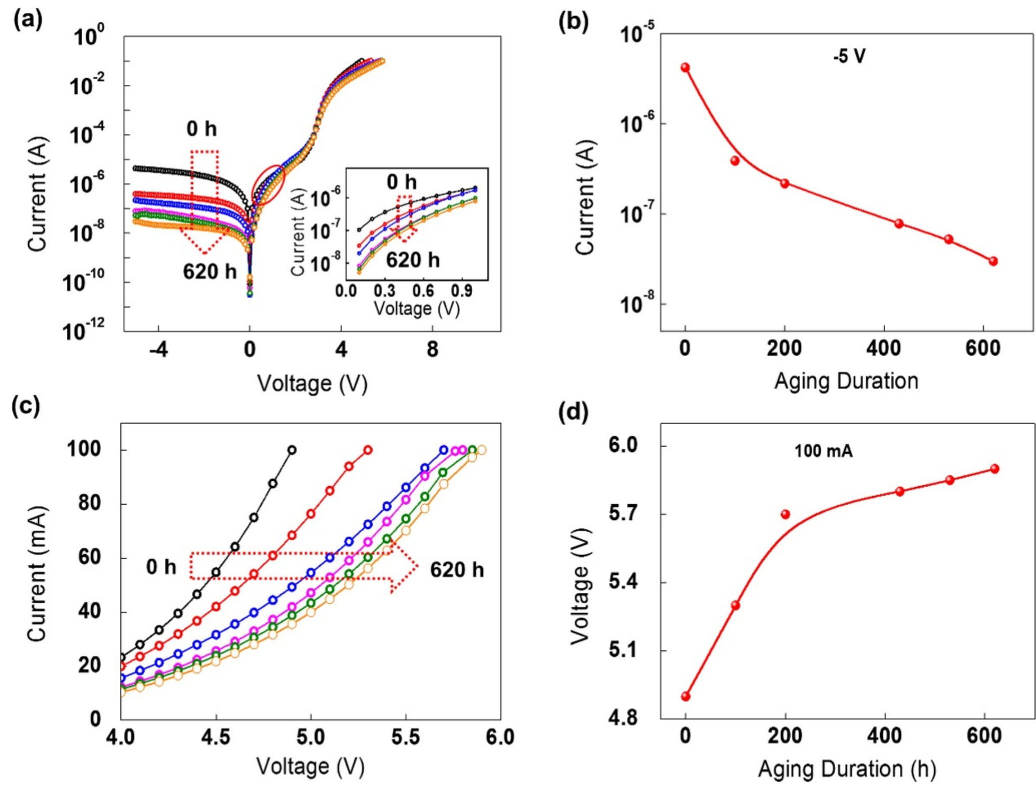

Figure 2. (a) The evolution of $I–V$ curves over aging duration, the inset shows the enlarged $I–V$ curves for the range of $0.1 \sim 1$ V. (b) The reverse leakage current at -5 V as a function of aging duration. (c) The enlarged $I–V$ curves for the range of $4 \sim 6$ V at various aging duration. (d) The operation voltage at 100 mA as a function of aging duration.

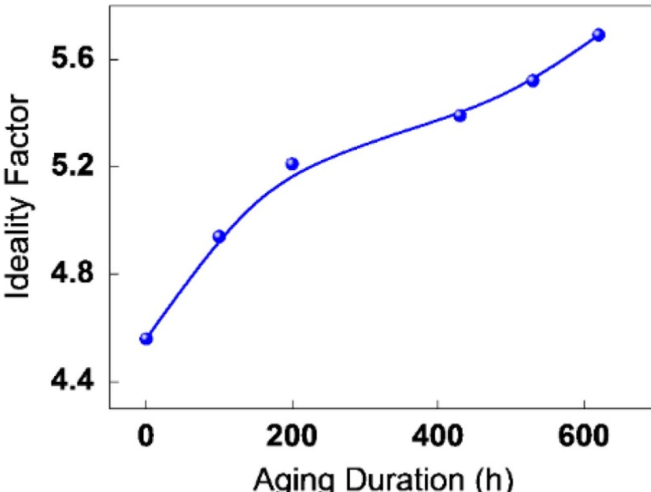

Figure 3. The ideality factor of the aged LD as a function of aging duration.

the light output power dropped by half, and the threshold current correspondingly increased from 75–100 mA, as shown in figure 1(b). However, the slope efficiency remained nearly unchanged.

$$\eta_{slope} = \eta_{inj} \frac{\alpha_m}{\alpha_m + \alpha_i} \frac{h\nu}{q}. \quad (1)$$

When the injection current of the LD is above threshold, the slope efficiency can be expressed by equation (1), where η_{inj}, α_m, α_i, $h\nu$ and q are the injection efficiency, mirror and internal losses, photon energy and electronic charge, respectively [13]. The little drop in slope efficiency indicates that the electric stress did not induce any significant change in mirror and internal losses, as well as carrier injection efficiency. In fact, this phenomenon has also been reported by other research groups [14, 15]. Figure 1(c) presents the spontaneous emission integral intensity of the LD under various injection current before and after aging. For the as-fabricated LD, the spontaneous emission intensity increased rapidly with the injection current. But for the aged LD, it increased very slowly. It should be noted that the spontaneous emission intensity of the aged LD was substantially lower than that of the as-fabricated LD before aging, which indicates that the internal quantum efficiency (IQE) dropped greatly during the aging. The IQE reduction was probably mainly due to the generation and/or migration of point defects (impurities, vacancies, or interstitials) in the LD, which worked as nonradiative recombination centers and reduced the spontaneous emission intensity [16, 17].

On the other hand, the evolution of electrical properties was shown in figure 2(a). During aging, both the reverse and forward leakage current of aged LD decreased, which is distinctly different from the reports [18, 19]. Figure 2(b) shows the reverse leakage current at a reverse bias of -5 V as a function of aging duration. The reverse leakage current of the as-fabricated LD was 4.2×10^{-6} A, but it dropped to

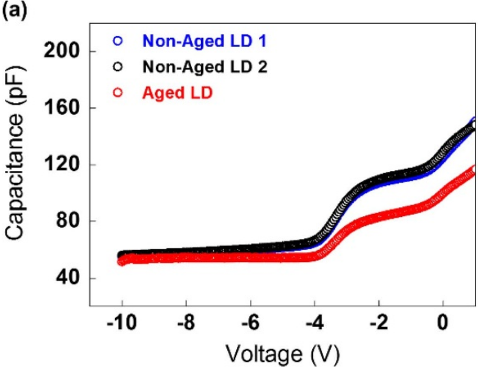

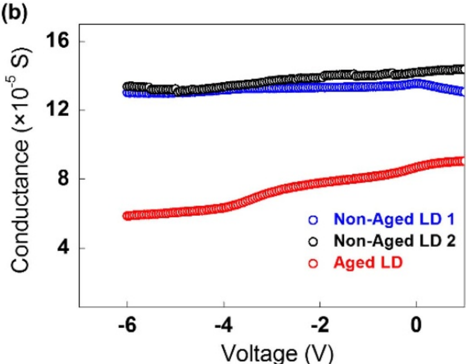

Figure 4. (a) The capacitance and (b) the conductance of the aged and neighboring as-fabricated LDs as a function of reverse bias voltage.

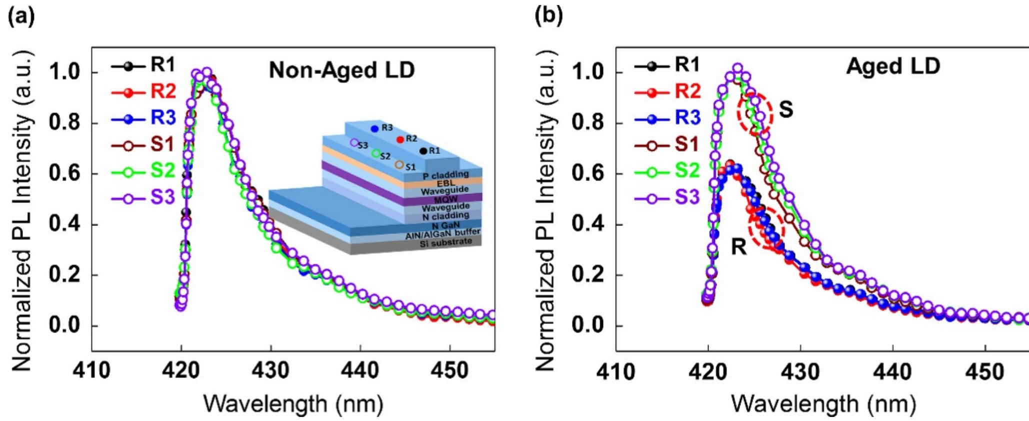

Figure 5. PL spectra of (a) aged LD and (b) neighboring as-fabricated LD, where R1, R2 and R3 indicate the excitation spots in the ridge region, while S1, S2 and S3 the excitation spots of the side region outside the ridge. The inset schematically showed the locations of R1, R2, R3, S1, S2 and S3.

3.0×10^{-8} A after aging for 620 h. The forward leakage current was also decreased with the aging duration, as shown in the inset of figure 2(a). Figure 2(c) shows the enlarged *I–V* curves for the range of 4 ∼ 6 V at various aging durations. With the aging duration increased, the series resistance of the LD increased greatly, and hence the operation voltage went up correspondingly. The operation voltage at 100 mA increased from 4.9–5.7 V after aging for 620 h, as shown in figure 2(d).

The measured *I–V* curves of the aged LDs can be fitted by the empirical diode equation, therefore, the ideality factor of the aged LD can be obtained according to the following formula [20].

$$n = \frac{q}{kT}\frac{dV}{d(\ln I)} \tag{2}$$

where q is the electronic charge, k the Boltzmann constant, and T the absolute temperature. Figure 3 shows the ideality factor of the aged LD as a function of aging duration. The ideality factor n of the as-fabricated LD was larger than 2 (n = 4.5), which has been often observed for GaN-based diodes due to the high barrier [20–23]. After aging, the ideality factor n of the InGaN-based LD increased from 4.5 to 5.7. It can be inferred that the carrier concentration decreased and hence the barrier height increased, which indicates that acceptor-like defects might generated in or around the active region under the electrical stress, compensating the electrons and reducing the net charge. It would increase width of the space-charge region. As a result, the series resistance increased, and hence the leakage current was reduced.

In order to locate the newly generated defects in the InGaN-based LD, the capacitance and conductance of the aged and neighboring as-fabricated LDs were measured, as shown in figure 4. When the bias voltage was in the range of −10 to −6 V, the capacitance of the aged LD was almost the same as that of the neighboring as-fabricated LDs. However, the capacitance of aged LD was much smaller than that of neighboring as-fabricated LDs, when the bias voltage was in the range of −6 – 1 V, especially around −2 V. The dopant concentration in the p-type materials, including p-type EBL (Mg: 1.5×10^{19} cm^{-3}) and cladding layer (Mg: 1.6×10^{19} cm^{-3}), was much higher than that in the n-type materials, including the unintentionally doped upper and lower waveguide layers, quantum wells, and n-type cladding layer (Si: 1.5×10^{18} cm^{-3}). It is well-known that the activation energy of Mg acceptors is much higher than that of Si donors in GaN, therefore only a few percent of the Mg dopants could be ionized at room temperature. However, due to the energy band bending caused by the strong electrical field during the *C-V* measurements, the activation percentage of the Mg acceptors

was significantly increased. Therefore, most of the Mg acceptors in p-side depletion region of the p-n junction could be ionized, which has also reported in other literature [24]. As a result, the depletion zone of the p-n junction mainly expanded in n-type region [25], and the *C-V* results revealed that the newly generated defects were mainly in the waveguide layers, quantum wells, and n-type cladding layer. At a reverse bias of around −2 V, the depletion region mainly located in or around the active region. Meanwhile, the conductance of the aged LD was much lower than that of the neighboring as-fabricated LDs (figure 4(b)), indicating that the carrier concentration was dramatically reduced after the aging process. It can be inferred that acceptor-like defects were formed in or around the active region during the aging, and these defects compensated the carriers in the depletion region of the aged LD, reducing the conductance and capacitance of the aged LD [24, 26, 27].

In order to verify the location of the newly generated defects in the aged LD, PL measurement of the active region was carried out at various spots in and outside of the ridge region of the LD. Figure 5 shows the PL spectra of aged LD and neighboring as-fabricated LD with the excitation located at various spots. For the neighboring as-fabricated LD, the PL intensity of the ridge region was nearly the same as that of the side region outside the ridge (figure 5(a)). However, for aged LD, the PL intensity of the ridge was reduced to only about 60% of that of the side region outside the ridge, as shown in figure 5(b), which proves that point defects were generated in the active region of the LD. These defects acted as non-radiative recombination centers, greatly reducing the PL intensity and IQE [28], which is consistent with the observation of spontaneous emission drop during the electroluminescence measurement below the threshold (figure 1(c)).

According to the previous reports [29, 30], group-III vacancies (V_{III}) have a low formation energy in n-type group-III nitride materials, and can act as compensating centers, reducing the electrical conductivity and increasing the operation voltage. As reported in the literature [31], the formation energy of Ga vacancy (V_{Ga}) and related complexes is high in defect-free GaN materials, but it decreases substantially in the presence of TDs for defective GaN. In some locations nearby the TDs, the formation energy of V_{Ga} and related complexes can even be negative, suggesting that it is feasible to generate V_{Ga}-related complexes around TDs. Moreover, due to large size of In atoms, the bond energy of In-N bond is a lot weaker than Ga-N, therefore In vacancies (V_{In}) are much easier to form, as compared to V_{Ga}. In fact, Li and Zhou *et al* already demonstrated that V_{III}-related defects are easy to generate around TDs [32, 33]. All these results indicate that threading dislocations can assist the formation of V_{III}. For the InGaN-based LDs grown on Si, there are still a relatively high density ($\sim 10^8$ cm^{-2}) of TDs in the epitaxial layer due to large mismatch in lattice constant between GaN and Si substrate, as compared to that of free-standing GaN substrate ($\sim 10^6$ cm^{-2} or below). Therefore, it is reasonable to assume the generation of V_{III}-related defects near the TDs in the active region of the LD under the applied electrical stress and the large residual mechanical stress during the aging process. The V_{III}-related defects, together with the pre-existing TDs, can act as Shockley-Read-Hall centers [34], causing non-radiative recombination and affecting the IQE of the active region of the InGaN-based LD grown on Si. The non-radiative recombination leads to heat accumulation and junction temperature rise, and hence further facilitates the LD degradation. These newly generated group-III vacancies and/or related complexes could not only compensate the carriers in or around the active region of the LD, reducing capacitance and reverse leakage current, but also act as non-radiative recombination centers, reducing IQE and spontaneous emission intensity. Further reduction of TDs and improvement of active region crystalline quality will be carried out to enhance the performance and lifetime of InGaN-based LDs grown on Si. Recently, we have successfully grown GaN film grown on Si with a dislocation density of 6×10^7 cm^{-2} [35]. By using this template, the lifetime of InGaN-based LDs grown on Si is expected to be greatly improved.

4. Conclusion

In summary, the degradation characteristics and possible mechanism causing degradation of InGaN-based LDs grown on Si substrate have been studied. After aging under an electrical stress, the threshold current and driving voltage of the LD increased significantly, while the light output power, leakage current, capacitance and spontaneous emission intensity decreased greatly. But the slope efficiency remain nearly unchanged. These observations indicate some defects were generated in or around the active region of the aged LD. Group-III vacancies and related defects were proposed to account for the degradation of the LD. It is assumed that the relatively high density of TDs in the InGaN-based LD grown on Si substrate assist the formation of group-III vacancies in the active region. These generated group-III vacancies not only acted as acceptor-like defects, compensating the carriers and reducing the conductance, but also played as non-radiative combination centers, affecting the IQE and light output power.

Acknowledgments

The authors are grateful for the financial support from the Key-Area R&D Program of Guangdong Province (Grant Nos. 2019B010130001 and 2019B090917005), the National Key R&D Program (Grant Nos. 2016YFB0400100 and 2016YFB0400104), the National Natural Science Foundation of China (Grant Nos. 61534007, 61775230, 61804162, and 61874131), the Strategic Priority Research Program of CAS (Grant Nos. XDB43000000 and XDB43020200), the Key Research Program of Frontier Sciences, CAS (Grant Nos. QYZDB-SSW-JSC014 and ZDBS-LY-JSC040), the CAS Interdisciplinary Innovation Team, the Key R&D Program of Jiangsu Province (Grant No. BE2017079), the Natural Science Foundation of Jiangsu Province (Grant No. BK20180253), the Natural Science Foundation of Jiangxi Province (Grant No. 20181ACB20002), the Suzhou Science and Technology Program (Grant Nos. SYG201846 and SYG201927), and the China Postdoctoral Science Foundation (Grant No.

2018M632408). This work was also supported by the Open Fund of the State Key Laboratory of Reliability and Intelligence of Electrical Equipment (Grant No. EERIKF2018001). We are thankful for the technical support from Nano Fabrication Facility, Platform for Characterization and Test, and Nano-X of SINANO, CAS.

ORCID iDs

Yongjun Tang https://orcid.org/0000-0002-3553-127X
Jianxun Liu https://orcid.org/0000-0001-8485-166X
Jin Wang https://orcid.org/0000-0003-3098-4138

References

[1] Chi Y-C, Hsieh D-H, Tsai C-T, Chen H-Y, Kuo H-C and Lin G-R 2015 *Opt. Express* **23** 13051
[2] Wu T-C, Chi Y-C, Wang H-Y, Tsai C-T and Lin G-R 2017 *Sci. Rep.* **7** 40480
[3] Miyoshi T, Kozaki T, Yanamoto T, Fujimura Y, Nagahama S and Mukai T 2007 *J. Soc. Inf. Disp.* **15** 157
[4] Kuritzky L Y and Speck J S 2015 *MRS Commun.* **5** 463
[5] Nakamura S *et al* 1998 *Appl. Phys. Lett.* **72** 2014
[6] Nakamura S, Senoh M, Nagahama S-I, Iwasa N, Yamada T, Matsushita T, Kiyoku H, Sugimoto Y, Kozaki T and Umemoto H 1998 *Japan. J. Appl. Phys.* **37** L309
[7] Hazari A, Aiello A, Tien-Khee N, Ooi B S and Bhattacharya P 2015 *Appl. Phys. Lett.* **107** 191107
[8] Hazari A, Bhattacharya A, Frost T, Zhao S, Baten M Z, Mi Z and Bhattacharya P 2015 *Opt. Lett.* **40** 3304
[9] Qian S, Wei Y, Meixin F, Zengcheng L, Bo F, Hanmin Z and Hui Y 2016 *J. Semicond.* **37** 044006
[10] Sun Y *et al* 2016 *Nat. Photon.* **10** 595
[11] Sun Y *et al* 2018 *Light Sci. Appl.* **7** 13
[12] Liu J *et al* 2019 *Opt. Express* **27** 25943
[13] Coldren L A, Corzine S W and Mašanović M L 1995 *Diode Lasers and Photonic Integrated Circuits* (New York: Wiley) (https://doi.org/10.1117/1.601191)
[14] Perlin P, Marona L, Leszczyński M, Suski T, Wiśniewski P, Czernecki R and Grzegory I 2010 *Proc. IEEE* **98** 1214
[15] Trivellin N, Meneghini M, Zanoni E, Orita K, Yuri M, Tanaka T and Ueda D 2010 *Proc. IEEE Int. Rel. Phys. Symp.* 1–6
[16] Orita K, Meneghini M, Ohno H, Trivellin N, Ikedo N, Takigawa S, Yuri M, Tanaka T, Zanoni E and Meneghesso G 2012 *IEEE J. Quantum Electron.* **48** 1169
[17] Trivellin N, Meneghini M, Zanoni E, Meneghesso G, Orita K, Yuri M, Tanaka T and Ueda D 2010 *Phys. Status Solidi* A **207** 41
[18] Wen P *et al* 2015 *J. Phys. D: Appl. Phys.* **48** 415101
[19] Wen P, Zhang S, Li D, Liu J, Zhang L, Shi D, Zhou K, Tian A, Feng S and Yang H 2016 *Superlattices Microstruct.* **99** 72
[20] Zhu D, Xu J, Noemaun A N, Kim J K, Schubert E F, Crawford M H and Koleske D D 2009 *Appl. Phys. Lett.* **94** 81113
[21] Shah J M, Li Y-L, Gessmann T and Schubert E F 2003 *J. Appl. Phys.* **94** 2627
[22] Chitnis A, Kumar A, Shatalov M, Adivarahan V, Lunev A, Yang J W, Simin G, Khan M A, Gaska R and Shur M 2000 *Appl. Phys. Lett.* **77** 3800
[23] Yan D, Lu H, Chen D, Zhang R and Zheng Y 2010 *Appl. Phys. Lett.* **96** 083504
[24] Glaab J *et al* 2018 *J. Appl. Phys.* **123** 104502
[25] Kim T-S *et al* 2012 *Appl. Phys. Lett.* **100** 71910
[26] Monti D *et al* 2017 *IEEE Trans. Electron Devices* **64** 200
[27] Glaab J *et al* 2019 *IEEE Photon. Tech. Lett.* **31** 529
[28] Wen P, Zhang S, Liu J, Li D, Zhang L, Sun Q, Tian A, Zhou K, Zhou T and Yang H 2016 *J. Appl. Phys.* **119** 213107
[29] Limpijumnong S and Van de Walle C G 2004 *Phys. Rev.* B **69** 035207
[30] Reshchikov M A and Hadis M 2005 *J. Appl. Phys.* **97** 61301
[31] Elsner J, Jones R, Heggie M I, Sitch P K, Haugk M, Frauenheim T, Őberg S and Briddon P R 1998 *Phys. Rev.* B **58** 19
[32] Li Z *et al* 2013 *Appl. Phys. Lett.* **103** 152109
[33] Zhou K *et al* 2017 *Proc. SPIE* **10244** 102441X
[34] Dreyer C E, Alkauskas A, Lyons J L, Speck J S and Van de Walle C G 2016 *Appl. Phys. Lett.* **108** 141101
[35] Liu J, Huang Y, Sun X, Zhan X, Sun Q, Gao H, Feng M, Zhou Y, Ikeda M and Yang H 2019 *J. Phys. D: Appl. Phys.* **52** 425102